Journal of Sound and Vibration 330 (2011) 757–770

Contents lists available at ScienceDirect

Journal of Sound and Vibration

journal homepage: www.elsevier.com/locate/jsvi

Structural damage identification for railway bridges based on train-induced bridge responses and sensitivity analysis

J.W. Zhan [a,c,*], H. Xia [a], S.Y. Chen [b], G. De Roeck [c]

[a] School of Civil Engineering, Beijing Jiaotong University, Beijing 100044, China
[b] Bridge Technology Development Center, CCCC Highway Consultants Co., Ltd., Beijing 100088, China
[c] Department of Civil Engineering, Catholic University of Leuven, Heverlee B3001, Belgium

ARTICLE INFO

Article history:
Received 1 April 2010
Received in revised form
15 August 2010
Accepted 23 August 2010
Handling Editor: M.P. Cartmell
Available online 20 September 2010

ABSTRACT

A damage identification approach using train-induced responses and sensitivity analysis is proposed for the nondestructive evaluation of railway bridges. The dynamic responses of railway bridges under moving trains composed of multiple vehicles are calculated by a train–bridge dynamic interaction analysis. Using the stiffness variation of the bridge element as an index for damage identification, the sensitivities of train-induced bridge responses to structural damage are analyzed and the sensitivity matrices are formed. By comparing the theoretical measurement responses of one measurement point in two different states, the damage indices of all elements are updated iteratively, and finally the absolute or relative damage is located and quantified. A three-span continuous bridge numerical example proves that the proposed dynamic response sensitivity-based FE model updating damage identification method is not only effective to detect local damage of railway bridges, but also insensitive to the track irregularity and the measurement noise.

1. Introduction

Damage in bridges can result in changes of their mechanical properties such as mass, stiffness, damping and boundary conditions, which can be reflected by changes in their global dynamic characteristics. The damage identification based on the global dynamic characteristics of structures has become currently a topic of very active research in civil and mechanical engineering. Various damage identification methods have been proposed by utilizing such parameters as natural frequencies [1,2], mode shapes [3,4], curvature mode shapes [5], modal damping [6], modal strain energies [7], frequency response functions [8] and stiffness or flexibility sensitivities [9,10]. Doebling et al. [11] comprehensively reviewed the literature, focusing on frequency-domain damage detection algorithms for linear structures. Zou et al. [12] summarized the methods on vibration-based damage detection and health monitoring for composite structures. Housner et al. [13] gave a good summary on state-of-the-art methods in control and health monitoring of civil engineering structures.

The fundamental principle of these methods is to compare the structural behavior in the damaged state with that in the undamaged state. In order to detect the damage locations and to determine the damage extents, it is necessary to model the undamaged state of the structure. A reliable method can be obtained by comparing the experimentally measured data

* Corresponding author at: Beijing Jiaotong University, School of Civil Engineering, Bridge Engineering Department, No. 3 Shang Yuan Cun, Hai Dian District, Beijing 100044, China. Tel.: +86 1051683786; fax: +86 1051683494.
E-mail address: jwzhan@bjtu.edu.cn (J.W. Zhan).

0022-460X/$ - see front matter © 2010 Elsevier Ltd. All rights reserved.
doi:10.1016/j.jsv.2010.08.031

of a structure in its initial state with those predicted by an initial mathematical model [14,15]. However, for an accurate model based damage assessment, often a lot of sensors and manual processing are needed, jeopardizing the online damage detection of structures in service.

From the view of structural online health monitoring, it is desirable to locate and quantify the damage directly from the time-domain dynamic responses of bridges under operating loads such as running vehicles. For this purpose, much research has been conducted. Liu and Chen [16] presented an inverse technique for identifying stiffness distribution in structures using the structural dynamic responses, where the sensitivity matrices of structural displacements with respect to the stiffness factors were calculated by Newton's method. Cattarius and Inman [17] detected the damage in smart structures from the time histories of structural responses. Chen and Li [18] and Shi et al. [19] proposed methods to identify both structural parameters and input loads from output-only measurements. Ling et al. [20] proposed an element level system identification method with unknown input with Rayleigh damping. Lu and Law [21, and Lu et al. [22] studied the features of dynamic response sensitivities under sinusoidal, impulsive and random excitations, and then used them in the structural damage identification. For large civil structures such as long-span bridges, it is usually difficult to excite them by impulsive or sinusoidal loads, so the passing vehicles are more suitable as excitation sources. Majumder and Manohar [23] proposed a time-domain approach for damage detection in bridges using both the vehicle response and the bridge response, in which the vehicle was considered as a single degree-of-freedom system with sprung and unsprung masses. Zhu and Law [24] studied the damage detection of simply supported concrete bridges, in which the moving forces and the damage indices are identified at the same time from the measured responses of multiple points.

In the above references, none is considering the damage detection of railway bridges from the dynamic responses due to passing trains composed of multiple vehicles. All papers also presume prior knowledge of the FE model in the undamaged state.

In this paper, a detailed train–bridge dynamic interaction model is established, in which the train is composed of multiple 4-axle vehicles with 10 degrees-of-freedom and the bridge is discretized by beam elements. The train-induced responses of the bridge in the damaged state are used as input data for damage identification and the response sensitivities with respect to the damage indices of the elements are calculated to establish the sensitivity matrix. Using the error between the measured response and the computed one as a minimization criterion, the sensitivity equation is solved by the least-squares method, and then the damage is located and quantified with the finite element model updating technique. In the proposed method, the influences of measurement noise and track irregularities on the analysis results are discussed. An example of a three-span continuous bridge numerical example proves that the local damage of railway bridges can be effectively identified using the train-induced response of a single measurement point.

2. Forward problem solution for train-induced bridge response

Since only the vertical response of the bridge is used in this study, a two-dimensional dynamic model of the train–bridge interaction system, composed of a train subsystem and a bridge subsystem, is established in the X–Z plane. The two subsystems are linked by the assumed wheel–track interactions.

The train subsystem model adopts the following assumptions:

(1) The train runs on the bridge at a constant speed.
(2) The train can be modeled as several independent vehicle elements. Each vehicle element is composed of a car body, two bogies, four wheel-sets and the spring–damper suspensions between the components.
(3) The car body, bogies and wheel-sets in each vehicle element are regarded as rigid components, neglecting their elastic deformations.
(4) The connections between a bogie and its wheel-sets are characterized by the first suspension system, which consists of springs and dampers with identical properties.
(5) The connections between a car body and its bogies are characterized by the second suspension system, which consists of springs and dampers with identical properties.
(6) The springs in vehicle elements are all linear, and the dampers all viscous.
(7) Each car body or bogie has 2 degrees-of-freedom in the Z and RY directions, while the longitudinal movement in the X direction is neglected.

Only the degree-of-freedom in the Z direction for the wheel-set is considered, thus each 4-axle vehicle element has 10 degrees-of-freedom (see Fig. 1).

Two-dimensional beam elements are used to model the bridge. In structural dynamics, the determination of the damping matrix is often difficult. The usual solution for this problem is to adopt the classical Rayleigh damping theory [25], in which the damping matrix $\mathbf{C}_b$ is expressed as a linear combination of the bridge mass matrix $\mathbf{M}_b$ and the stiffness matrix $\mathbf{K}_b$:

$$\mathbf{C}_b = \alpha\mathbf{M}_b + \beta\mathbf{K}_b \tag{1}$$

with $\alpha = 4\pi((\xi_1 f_1 f_2^2 - \xi_2 f_1^2 f_2)/(f_2^2 - f_1^2))$; $\beta = (1/\pi)((\xi_2 f_2 - \xi_1 f_1)/(f_2^2 - f_1^2))$.where f_1 and f_2 are the first- and the second-order natural frequencies (Hz). ξ_1 and ξ_2 are the first- and the second-order damping ratios of the bridge, respectively.

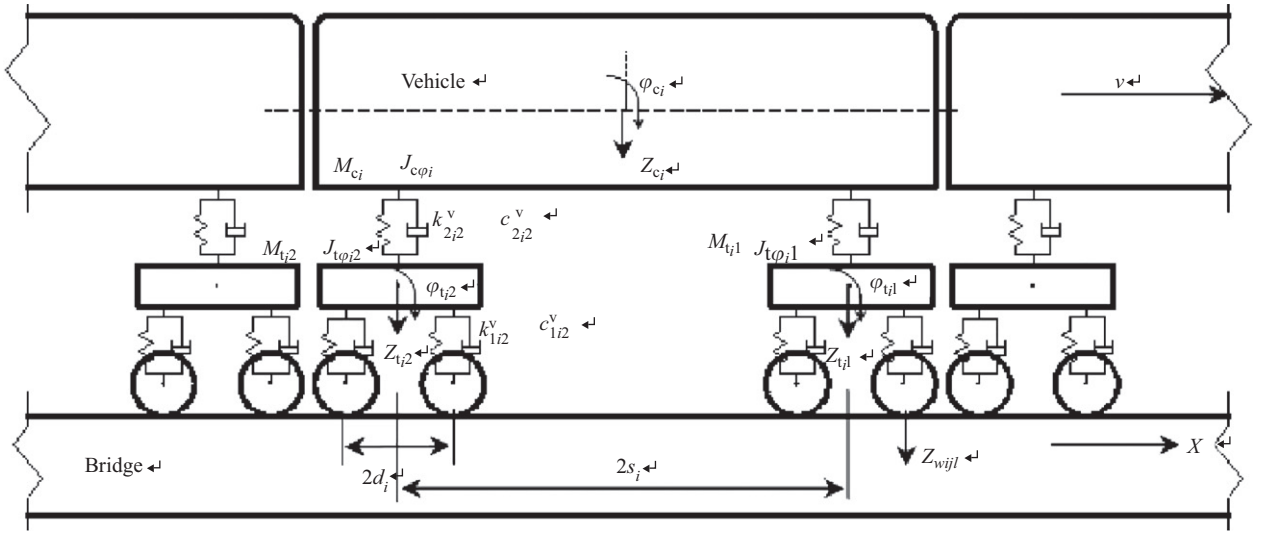

Fig. 1. Train–bridge interaction model.

In theory, any two natural frequencies can be used to calculate α and β. Usually in practice, the high-order frequencies are difficult to measure, while the low-order frequencies can be obtained precisely, therefore the first- and the second-order natural frequencies are used to calculate the combination coefficients α and β.

In the vehicle–bridge interaction dynamics, one of the assumptions is that the wheel-sets never detach from the bridge and the only connection between them is the track irregularity. The movements of the wheel-sets and the bridge couple together through the track irregularity with the following equations:

$$Z_{wijl} = Z_b(x_{ijl}) + Z_s(x_{ijl}) \tag{2a}$$

$$\dot{Z}_{wijl} = \dot{Z}_b(x_{ijl}) + \dot{Z}_s(x_{ijl}) \tag{2b}$$

$$\ddot{Z}_{wijl} = \ddot{Z}_b(x_{ijl}) + \ddot{Z}_s(x_{ijl}) \tag{2c}$$

where x_{ijl} is the position of the lth wheel-set of the jth bogie in the ith vehicle, Z_b, $\dot{Z}_b(x_{ijl})$ and $\ddot{Z}_b(x_{ijl})$ are, respectively, the displacement, velocity and acceleration of the bridge; $\underline{Z}_w$, $\dot{Z}_w$ and $\ddot{Z}_w$ are, respectively, the displacement, velocity and acceleration of the wheel-set; Z_s, $\dot{Z}_s$ and $\ddot{Z}_s$ are, respectively, the displacement, velocity and acceleration irregularities of the track on the bridge. Their computation method is described in Section 6.2.

The equations of the coupled motion of the train–bridge system can be expressed as

$$\begin{bmatrix} \mathbf{M}_{vv} & \mathbf{0} \\ \mathbf{0} & \mathbf{M}_{bb} \end{bmatrix} \begin{Bmatrix} \ddot{\mathbf{X}}_v \\ \ddot{\mathbf{X}}_b \end{Bmatrix} + \begin{bmatrix} \mathbf{C}_{vv} & \mathbf{C}_{vb} \\ \mathbf{C}_{bv} & \mathbf{C}_{bb} \end{bmatrix} \begin{Bmatrix} \dot{\mathbf{X}}_v \\ \dot{\mathbf{X}}_b \end{Bmatrix} + \begin{bmatrix} \mathbf{K}_{vv} & \mathbf{K}_{vb} \\ \mathbf{K}_{bv} & \mathbf{K}_{bb} \end{bmatrix} \begin{Bmatrix} \mathbf{X}_v \\ \mathbf{X}_b \end{Bmatrix} = \begin{Bmatrix} \mathbf{F}_v \\ \mathbf{F}_b \end{Bmatrix} \tag{3}$$

where $\mathbf{M}_{vv}$, $\mathbf{K}_{vv}$ and $\mathbf{C}_{vv}$ are, respectively, the mass, stiffness and damping matrices of the train; $\mathbf{C}_{vb}$, $\mathbf{K}_{vb}$, $\mathbf{C}_{bv}$ and $\mathbf{K}_{bv}$ are, respectively, the train–bridge interaction matrices; $\mathbf{X}_v$ and $\mathbf{X}_b$ are, respectively, the displacement vectors of the train and the bridge; $\mathbf{F}_v$ and $\mathbf{F}_b$ are, respectively, the force vectors acting on the train and the bridge. The computation of these matrices is described in detail by Xia and Zhang [26], and Zhang et al. [27].

Due to the coupling effects between the wheel-sets and the bridge, the generalized stiffness and damping matrices of the bridge, as deducted by Xia and Zhang [26], can be written as follows:

$$\begin{aligned} \mathbf{K}_{bb} = \mathbf{K}_b + \mathbf{K}^* = \mathbf{K}_b + \sum_{i=1}^{N_v} \sum_{j=1}^{2} \sum_{l=1}^{N_{wi}} \{ & m_{wijl} v^2 \mathbf{H}^{\mathrm{T}}(x_{ijl}) \mathbf{H}_{xx}(x_{ijl}) + m_{wijl} a \mathbf{H}^{\mathrm{T}}(x_{ijl}) \mathbf{H}_x(x_{ijl}) \\ & + k^v_{1ij} \mathbf{H}^{\mathrm{T}}(x_{ijl}) \mathbf{H}(x_{ijl}) + c^v_{1ij} v \mathbf{H}^{\mathrm{T}}(x_{ijl}) \mathbf{H}_x(x_{ijl}) \} \end{aligned} \tag{4}$$

$$\mathbf{C}_{bb} = \mathbf{C}_b + \mathbf{C}^* = \mathbf{C}_b + \sum_{i=1}^{N_v} \sum_{j=1}^{2} \sum_{l=1}^{N_{wi}} [2 m_{wijl} v \mathbf{H}^{\mathrm{T}}(x_{ijl}) \mathbf{H}_x(x_{ijl}) + c^v_{1ij} \mathbf{H}^{\mathrm{T}}(x_{ijl}) \mathbf{H}(x_{ijl}) \tag{5}$$

where $\mathbf{K}^*$ and $\mathbf{C}^*$ are, respectively, the additional stiffness and damping matrices of the wheel-sets on the bridge; $\mathbf{H}(x)$ is the interpolation function matrix [28]; $\mathbf{H}_x$ and $\mathbf{H}_{xx}$ denote the first and the second derivative with respect to x of $\mathbf{H}(x)$, respectively; v and a are the moving speed and the moving acceleration of the train in the X direction, respectively; m_{wijl} is

the mass of the wheel-set; k_{1ij}^{v} and c_{1ij}^{v} are the spring coefficient and the damping coefficient of the first suspension system, respectively; N_v is the total number of vehicles in the train; N_{wi} is the total number of wheel-sets of each bogie.

When the model parameters and the external forces are known, the computation of the bridge responses is a forward problem [26]. Eq. (3) can be solved by the Newmark direct integration method. The displacement, velocity and acceleration responses of location x at time t can be interpolated from the computed nodal responses.

3. Dynamic response sensitivity analysis

3.1. Damage index definition

Except for some special cases, it is usually assumed that damage does not change the mass but the stiffness of the structure [11]. The damage index of the bridge can be defined as the relative reduction ratio of the element stiffness. If the relative damage index and the stiffness of the jth element in the reference state are, respectively, α^j and$(\mathrm{EI})^j_{\mathrm{refer}}$, its stiffness in the damaged state can be expressed as

$$(\mathrm{EI})_d{}^j = (\mathrm{EI})^j_{\mathrm{refer}}(1-\alpha^j) \quad (0 \le \alpha^j \le 1, j = 1,2,\ldots,N) \tag{6}$$

where N is the total number of the bridge elements.

3.2. Sensitivity of response with respect to damage index

For a perturbation of the system parameters, the perturbed equation of motion is obtained by differentiating both sides of Eq. (3) with respect to the system parameter [22]. Assuming the damage index is related only to the stiffness of the dynamic system, the following differentiation equation can be obtained:

$$\begin{aligned}&\frac{\partial}{\partial\alpha^j}\left\{\begin{bmatrix}\mathbf{M}_{vv} & \mathbf{0}\\ \mathbf{0} & \mathbf{M}_{bb}\end{bmatrix}\right\}\left\{\ddot{\mathbf{X}}_v\ddot{\mathbf{X}}_b\right\}+\frac{\partial}{\partial\alpha^j}\left\{\begin{bmatrix}\mathbf{C}_{vv} & \mathbf{C}_{vb}\\ \mathbf{C}_{bv} & \mathbf{C}_{bb}\end{bmatrix}\right\}\left\{\dot{\mathbf{X}}_v\dot{\mathbf{X}}_b\right\}+\frac{\partial}{\partial\alpha^j}\left\{\begin{bmatrix}\mathbf{K}_{vv} & \mathbf{K}_{vb}\\ \mathbf{K}_{bv} & \mathbf{K}_{bb}\end{bmatrix}\right\}\begin{Bmatrix}\mathbf{X}_v\\ \mathbf{X}_b\end{Bmatrix}\\ &+\begin{bmatrix}\mathbf{M}_{vv} & \mathbf{0}\\ \mathbf{0} & \mathbf{M}_{bb}\end{bmatrix}\begin{Bmatrix}\partial\dfrac{\ddot{\mathbf{X}}_v}{\partial(\alpha^j)}\\ \partial\dfrac{\ddot{\mathbf{X}}_b}{\partial(\alpha^j)}\end{Bmatrix}+\begin{bmatrix}\mathbf{C}_{vv} & \mathbf{C}_{vb}\\ \mathbf{C}_{bv} & \mathbf{C}_{bb}\end{bmatrix}\begin{Bmatrix}\partial\dfrac{\dot{\mathbf{X}}_v}{\partial(\alpha^j)}\\ \partial\dfrac{\dot{\mathbf{X}}_b}{\partial(\alpha^j)}\end{Bmatrix}+\begin{bmatrix}\mathbf{K}_{vv} & \mathbf{K}_{vb}\\ \mathbf{K}_{bv} & \mathbf{K}_{bb}\end{bmatrix}\begin{Bmatrix}\dfrac{\partial\mathbf{X}_v}{\partial(\alpha^j)}\\ \dfrac{\partial\mathbf{X}_b}{\partial(\alpha^j)}\end{Bmatrix}=\frac{\partial}{\partial\alpha^j}\begin{Bmatrix}\mathbf{F}_v\\ \mathbf{F}_b\end{Bmatrix}\end{aligned} \tag{7}$$

It can be seen from Eqs. (4) and (5) that $\mathbf{K}^*$ and $\mathbf{C}^*$ are independent of α^j, and $\mathbf{M}_{bb}$, $\mathbf{M}_{vv}$, $\mathbf{C}_{vv}$, $\mathbf{K}_{vv}$, $\mathbf{C}_{vb}$, $\mathbf{K}_{vb}$, $\mathbf{C}_{bv}$, $\mathbf{K}_{bv}$, $\mathbf{F}_b$ and $\mathbf{F}_v$ are independent of α^j [26], so the following equations are valid, when considering Eq. (1):

$$\frac{\partial\mathbf{K}_{bb}}{\partial\alpha^j} = \frac{\partial\mathbf{K}_b}{\partial\alpha^j} \tag{8a}$$

$$\frac{\partial\mathbf{C}_{bb}}{\partial\alpha^j} = \frac{\partial\mathbf{C}_b}{\partial\alpha^j} = \beta\frac{\partial\mathbf{K}_b}{\partial\alpha^j} \tag{8b}$$

Then Eq. (7) can be simplified as

$$\begin{bmatrix}\mathbf{M}_{vv} & \mathbf{0}\\ \mathbf{0} & \mathbf{M}_{bb}\end{bmatrix}\begin{Bmatrix}\partial\dfrac{\ddot{\mathbf{X}}_v}{\partial(\alpha^j)}\\ \partial\dfrac{\ddot{\mathbf{X}}_b}{\partial(\alpha^j)}\end{Bmatrix}+\begin{bmatrix}\mathbf{C}_{vv} & C_{vb}\\ \mathbf{C}_{bv} & \mathbf{C}_{bb}\end{bmatrix}\begin{Bmatrix}\partial\dfrac{\dot{\mathbf{X}}_v}{\partial(\alpha^j)}\\ \partial\dfrac{\dot{\mathbf{X}}_b}{\partial(\alpha^j)}\end{Bmatrix}+\begin{bmatrix}\mathbf{K}_{vv} & K_{vb}\\ \mathbf{K}_{bv} & \mathbf{K}_{bb}\end{bmatrix}\begin{Bmatrix}\dfrac{\partial\mathbf{X}_v}{\partial(\alpha^j)}\\ \dfrac{\partial\mathbf{X}_b}{\partial(\alpha^j)}\end{Bmatrix}=\begin{Bmatrix}\mathbf{0}\\ -\dfrac{\partial\mathbf{K}_b}{\partial(\alpha^j)}\mathbf{X}_b-\beta\dfrac{\partial\mathbf{K}_b}{\partial(\alpha^j)}\dot{\mathbf{X}}_b\end{Bmatrix} \quad (j = 1,2,\ldots,N) \tag{9}$$

It can be observed that the velocity response $\dot{\mathbf{X}}_b$ and the displacement response $\mathbf{X}_b$, obtained from Eq. (3), are the input data for Eq. (9). As a forward problem, the response sensitivities of the nodes can also be obtained from Eq. (9) by the Newmark direct integration method. The response sensitivities of any point with coordinate x can be computed by the following equations:

$$\frac{\partial\mathrm{u}(x,t)}{\partial(\alpha^j)} = \mathbf{H}(\mathrm{x})\frac{\partial\mathbf{X}_b}{\partial(\alpha^j)} \tag{10a}$$

$$\frac{\partial\dot{\mathrm{u}}(x,t)}{\partial(\alpha^j)} = \mathbf{H}(\mathrm{x})\partial\frac{\dot{\mathbf{X}}_b}{\partial(\alpha^j)} \tag{10b}$$

$$\frac{\partial\ddot{\mathrm{u}}(x,t)}{\partial(\alpha^j)} = \mathbf{H}(\mathrm{x})\partial\frac{\ddot{\mathbf{X}}_b}{\partial(\alpha^j)} \tag{10c}$$

4. Inverse problem solution for damage index vector

The identification problem is to find the damage index vector $\mathbf{A}=\{\alpha^1,\alpha^2,\ldots,\alpha^j,\ldots,\alpha^N\}^{\mathrm{T}}$ of the system based on the condition that the calculated responses best match the measured ones. The identification procedure is as follows:

Step 1: Update the reference finite element model of the bridge with the identified damage index vector $\mathbf{A}_k$ of the kth iteration step (the initial damage is usually assumed to be zero, i.e. $\mathbf{A}_1=\mathbf{0}$), to get $(\mathbf{K}_b)_k$ and $\partial(\mathbf{K}_b)_k/\partial\alpha_k^j$. The displacement response vector $(\mathbf{X}_b)_k$ and the velocity response vector $(\dot{\mathbf{X}}_b)_k$ can be calculated by Eq. (3). By substituting $(\mathbf{X}_b)_k$, $(\dot{\mathbf{X}}_b)_k$ and $\partial(\mathbf{K}_b)_k/\partial\alpha_k^j$ into Eq. (9), $(\partial\mathbf{X}_b/\partial\alpha_k^j)_k$ can be calculated.

Step 2: Calculate the response $\mathrm{u}_s^k(\mathrm{t_i})$ of the sth ($s=1,2,\ldots,\mathrm{NP}$) measurement point at the ith ($i=1,\ldots,\mathrm{NM}$) time step and its sensitivity $\frac{\partial \mathrm{u}_s^k(\mathrm{t_i})}{\partial\alpha_k^j}$ by interpolation from the nodal ones. Then construct the time-varying sensitivity matrix

$$\mathbf{S}_s^k=\begin{bmatrix} \frac{\partial \mathrm{u}_s^k(\mathrm{t}_1)}{\partial\alpha_k^1} & \frac{\partial \mathrm{u}_s^k(\mathrm{t}_1)}{\partial\alpha_k^2} & \cdots & \frac{\partial \mathrm{u}_s^k(\mathrm{t}_1)}{\partial\alpha_k^N} \\ \frac{\partial \mathrm{u}_s^k(\mathrm{t}_2)}{\partial\alpha_k^1} & \frac{\partial \mathrm{u}_s^k(\mathrm{t}_2)}{\partial\alpha_k^2} & \cdots & \frac{\partial \mathrm{u}_s^k(\mathrm{t}_2)}{\partial\alpha_k^N} \\ \vdots & \vdots & \cdots & \vdots \\ \frac{\partial \mathrm{u}_s^k(\mathrm{t_i})}{\partial\alpha_k^1} & \frac{\partial \mathrm{u}_s^k(\mathrm{t_i})}{\partial\alpha_k^2} & \cdots & \frac{\partial \mathrm{u}_s^k(\mathrm{t_i})}{\partial\alpha_k^N} \\ \vdots & \vdots & \cdots & \vdots \\ \frac{\partial \mathrm{u}_s^k(\mathrm{t_{NM}})}{\partial\alpha_k^1} & \frac{\partial \mathrm{u}_s^k(\mathrm{t_{NM}})}{\partial\alpha_k^2} & \cdots & \frac{\partial \mathrm{u}_s^k(\mathrm{t_{NM}})}{\partial\alpha_k^N} \end{bmatrix}_{\mathrm{NM}\times\mathrm{N}} \tag{11}$$

where NM is the total number of time steps and NP is the total number of measurement points.

Using the penalty function method [29], the sensitivity equation for damage identification can be expressed as

$$\mathbf{S}_s^k\times\Delta\mathbf{A}_k=\Delta\mathbf{U}_s^k \tag{12}$$

where $\Delta\mathbf{A}_k=\{\Delta\alpha_k^1,\ldots,\Delta\alpha_k^j,\ldots,\Delta\alpha_k^N\}^{\mathrm{T}}$ is the perturbation in the damage index vector at the kth iteration step; $\Delta\mathbf{U}_s^k=\{u_s^k(t_1)-\hat{u}_s^k(t_1),\ldots,u_s^k(t_i)-\hat{u}_s^k(t_i),\ldots,u_s^k(t_{\mathrm{NM}})-\hat{u}_s^k(t_{\mathrm{NM}})\}^{\mathrm{T}}$ is the discrepancy between the calculated displacement responses and the measured ones; the superscript ^ denotes the measured responses.

In theory, the sensitivity matrix of any single measurement point can be used for identification. For a bridge structure with N elements, the used response number NM must be far bigger than N to make sure that the set of Eq. (12) is overdetermined. Eq. (12) can be solved by the least-squares method

$$\Delta\mathbf{A}_k=[(\mathbf{S}_s^k)^{\mathrm{T}}\mathbf{S}_s^k]^{-1}(\mathbf{S}_s^k)^{\mathrm{T}}\Delta\mathbf{U}_s^k \tag{13}$$

Like many other inverse problems, Eq. (13) is an ill-conditioned system of equations and the solution is unstable. In order to provide bounds to the solution, the damped least-squares method developed by Tikhonov [30] and the singular value decomposition technique are used in the pseudo-inverse calculation. Eq. (13) can be written in the following form:

$$\Delta\mathbf{A}_k=[(\mathbf{S}_s^k)^{\mathrm{T}}\mathbf{S}_s^k+\lambda\mathbf{I}]^{-1}(\mathbf{S}_s^k)^{\mathrm{T}}\Delta\mathbf{U}_s^k \tag{14a}$$

where λ is the non-negative damping coefficient governing the participation of least-squares error in the solution. The solution of Eq. (14a) is equivalent to minimizing the function

$$J(\Delta\mathbf{A}_k,\lambda)=\|\mathbf{S}_s^k\Delta\mathbf{A}_k-\Delta\mathbf{U}_s^k\|^2+\lambda\|\Delta\mathbf{A}_k\|^2 \tag{14b}$$

where the second term in Eq. (14b) provides bounds to the solution. When the parameter λ approaches zero, the estimated vector $\Delta\mathbf{A}_k$approaches the solution obtained from the simple least-squares method.

Many methods, for example, the L-curve method, have been developed to get the regularization parameter λ. Hansen [31] designed a free Matlab package for analysis and solution of the discrete ill-posed problems basing on the L-curve method. This method is here used to obtain the optimal regularization parameter λ.

Once the increment in the damage index vector is obtained from Eq. (14a), the updated damage index vector can be expressed as

$$\mathbf{A}_{k+1}=\mathbf{A}_k+\Delta\mathbf{A}_k \tag{15}$$

Step 3: Repeat steps 1 and 2 to get the final value of the damage index vector. The following convergence criterion is used:

$$\|\mathbf{A}_{k+1}-\mathbf{A}_k\|/\|\mathbf{A}_{k+1}\|\le\varepsilon \tag{16}$$

where $\|\cdot\|$means the norm of a vector, $\varepsilon$is the allowable error (%).

For velocity or acceleration responses, the damage identification procedures are similar when the corresponding sensitivity matrices are properly constructed.

5. Train-induced response analysis of a damaged simply supported beam

A simply supported beam is used to analyze the influence of damage on the train-induced dynamic responses. As shown in Fig. 2, the bridge is discretized into 15 beam elements. The parameters of the simply supported bridge are length 30 m, Young's modulus E=35.5 GPa, sectional area A=2.0 m^2, moment of inertia I=1.4 m^4 and mass per unit length $\overline{m}=16{,}000\,\mathrm{kg}/m$.

The train used in the analysis consists of 4 identical vehicles whose parameters are shown in Table 1. In theory, the evaluation procedure is effective if the train speed is the same before and after the bridge is damaged. Acceleration, deceleration or moving at constant speed should be the same in both cases. However, for the ease of operation, the passing speed of the train is usually controlled to be constant. In the present analysis, the train runs onto the bridge from the left support and passes it at a constant speed of 30 m/s.

The natural frequencies of the car body and the bogie can be estimated from the following equations [32] as 1.05 and 6.38 Hz, respectively.

$$f_{\mathrm{vehicle}}=\frac{1}{2\pi}\sqrt{\frac{2}{\frac{(1/k_2^v)+(1/2k_1^v)}{M_c}}}=\frac{1}{\pi}\sqrt{\frac{M_c k_2^v k_1^v}{2k_1^v+k_2^v}} \tag{17}$$

$$f_{\mathrm{bogie}}=\frac{1}{2\pi}\sqrt{\frac{2k_1^v+k_2^v}{M_t}} \tag{18}$$

where is M_c and M_t are the mass of the car body and the bogie, k_1^v and k_2^v are the spring coefficients of the first- and the second-suspension system, respectively.

The elements of the bridge are assumed to successively suffer single damage with extents between 5% and 30%. At each damage case, the dynamic responses of the bridge are calculated based on the train–bridge dynamic interaction model.

Shown in Figs. 3 and 4 are the displacement and the acceleration responses of the bridge midpoint when element 8 suffers different extents of damage. The distribution of maximum displacements of the bridge midpoint with respect to element damage extent is shown in Fig. 5.

Fig. 3 shows that the midpoint displacements of the bridge increase when element 8 is more seriously damaged. However, the differences between the accelerations before and after the damage are less obvious (see Fig. 4).

For the single damage case, the following observations can be made from Fig. 5:

(1) The maximum displacements of the bridge increase when the damage extends.
(2) When the damage extent keeps unchanged, the maximum displacement decreases with the distance of the damaged element to the midpoint.
(3) For two elements symmetrically located to the midpoint, the same damage causes the same maximum displacement of the midpoint.

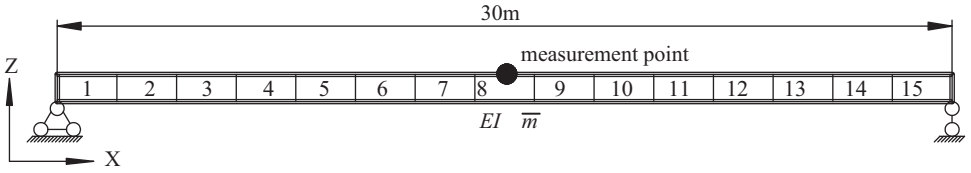

Fig. 2. Layout of the simply supported bridge model.

Table 1
Main parameters of the train vehicle used in the case study.

Item	Unit	Value
Full length of vehicle (L)	m	22.5
Distance of bogie ($2s$)	m	15.6
Distance of two wheel-sets ($2d$)	m	2.5
Mass of vehicle body (M_c)	kg	40,990
Mass of bogie (M_t)	kg	4360
Mass of wheel-set (M_w)	kg	1770
Vertical stiffness of 1st suspension system (k_1^v)	kN m^{-1}	2976
Vertical stiffness of 2nd suspension system (k_2^v)	kN m^{-1}	1060
Vertical damping of 1st suspension system (c_1^v)	kN s m^{-1}	15
Vertical damping of 2nd suspension system (c_2^v)	kN s m^{-1}	30
Mass moment of inertia of car body around the Y-axis ($J_{c\varphi}$)	kg m^2	1,959,000
Mass moment of inertia of bogie around the Y-axis ($J_{t\varphi}$)	kg m^2	1470

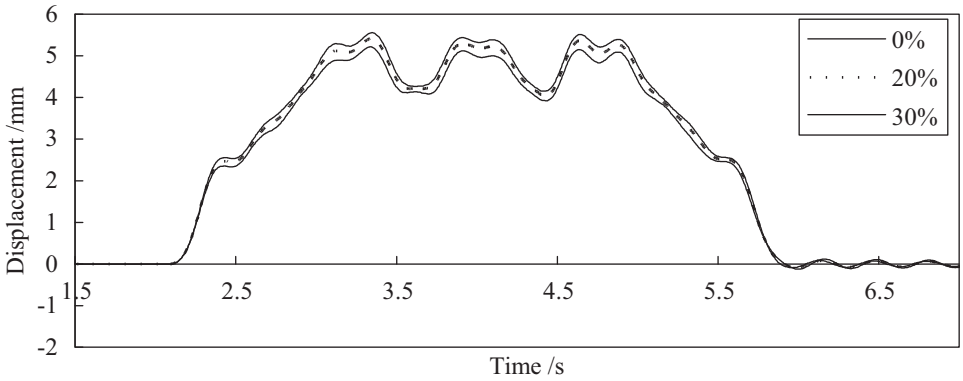

Fig. 3. Displacement responses of the midpoint when element 8 suffers different levels of damage.

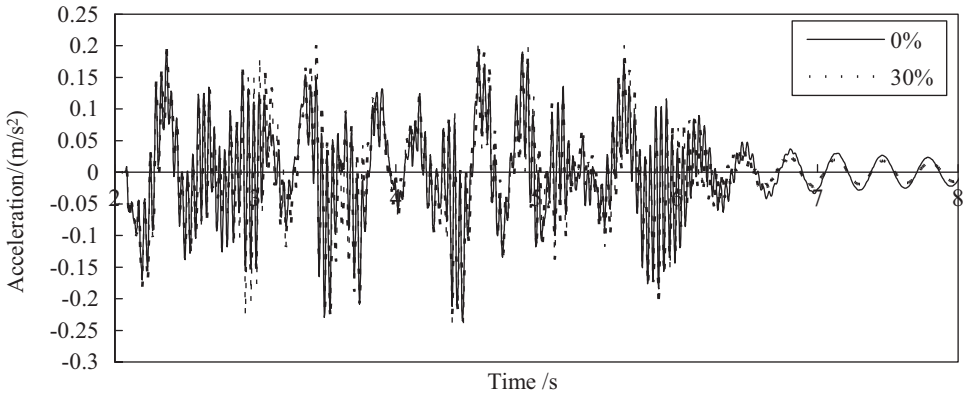

Fig. 4. Acceleration responses of the midpoint when element 8 suffers different levels of damage.

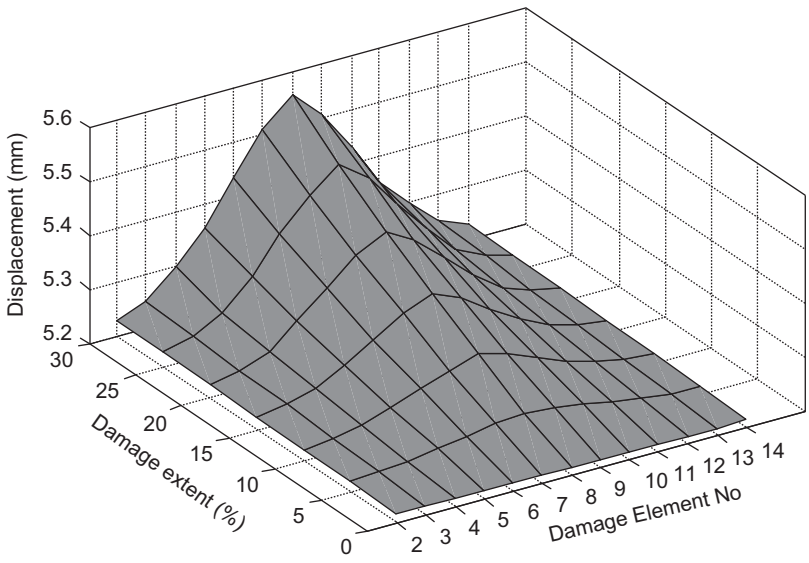

Fig. 5. Maximum displacements of the midpoint under different damage cases.

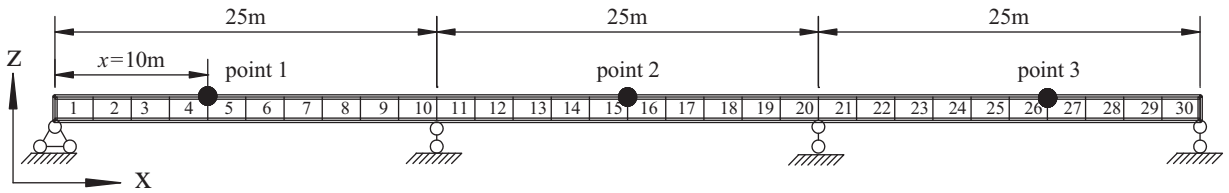

Fig. 6. Layout of the continuous bridge model.

6. Numerical example of damage identification

6.1. Model layout

A three-span continuous bridge with spans of 25 m+25 m+25 m (see Fig. 6) is studied to illustrate the feasibility and the efficiency of the proposed damage identification method. The bridge consists of 30 beam elements and 31 nodes, with each node having 3 degrees-of-freedom. The parameters of the bridge are Young's modulus E=35.5 GPa, sectional area A=3.0 m^2, moment of inertia I=0.84 m^4, and mass per unit length$\overline{m}=15{,}000\,\mathrm{kg}/m$. The same train as in Section 5 is used, which runs onto the bridge from the left support and passes it at a constant speed of 20 m/s.

6.2. Measurement noise, track irregularity and identification error

The normally distributed random noise is added to the calculated response of the bridge to simulate the measurement noise [21]

$$y_m = y_c + e_p N_0 \sigma(y_c) \tag{19}$$

where is the y_m and y_c are the polluted response and the calculated one, respectively, e_p is the ratio of noise amplitude to the response amplitude (between 0 and 1), N_0 is the standard normal distribution vector with a mean value of zero and a unit standard deviation, $\sigma(y_c)$is the standard deviation of the calculated response time history, which indicates the deviation of the response from its mean value. That is, if the mean value of the response is zero, $\sigma(y_c)$ denotes the amplitude of the response.

The track irregularity is introduced in Eq. (2) to link the displacements of the wheel-set and the bridge. In the United States, the track irregularity spectra are divided into 6 grades [33]. The vertical displacement, velocity and acceleration track irregularities are given by the following equations [26]:

$$\mathrm{Z}_s(\mathrm{x}) = \sum_{\mathrm{i}=1}^{\mathrm{n}_s} \sqrt{2\mathrm{S}_v(\Omega_\mathrm{i})\Delta\Omega}\cos(\Omega_\mathrm{i}\mathrm{x}+\phi_\mathrm{i}) \tag{20a}$$

$$\dot{\mathrm{Z}}_s(\mathrm{x}) = \sum_{\mathrm{i}=1}^{\mathrm{n}_s} -\sqrt{2\mathrm{S}_v(\Omega_\mathrm{i})\Delta\Omega}\Omega_\mathrm{i}\mathrm{v}\sin(\Omega_\mathrm{i}\mathrm{x}+\phi_\mathrm{i}) \tag{20b}$$

$$\ddot{\mathrm{Z}}_s(\mathrm{x}) = \sum_{\mathrm{i}=1}^{\mathrm{n}_s} -\sqrt{2\mathrm{S}_v(\Omega_\mathrm{i})\Delta\Omega}\Omega_\mathrm{i}^2\mathrm{v}^2\cos(\Omega_\mathrm{i}\mathrm{x}+\phi_\mathrm{i}) \tag{20c}$$

where is the φ_i is the random uniform-distribution phase between 0 and 2π;n_s is the total number of harmonic functions, x is the location of the wheel-set, Ω_1 and Ω_u are, respectively, the lower and the upper bounds of the spatial angular frequencies (rad/m), $\Delta\Omega=(\Omega_u-\Omega_l)/n_s$, $\Omega_i=\Omega_1+(i-1)\Delta\Omega$.

The power spectrum density is expressed as

$$\mathrm{S}_\mathrm{v}(\Omega) = \frac{\mathrm{k}\mathrm{A}_v\Omega_c^2}{\Omega^2(\Omega^2+\Omega_c^2)} \tag{21}$$

where k is the safety coefficient, A_v is the roughness coefficient and Ω_c is the cut-off frequency (rad/m).

The relative error (RE) is used to evaluate the precision of the identified damage extent. It is defined as

$$\mathrm{RE} = \|\mathbf{A}_\mathrm{id}-\mathbf{A}_r\|/\|\mathbf{A}_r\| \tag{22}$$

where $\mathbf{A}_\mathrm{id}$ and $\mathbf{A}_r$ are the identified damage index vector and the real one, respectively.

RE is an effective index to evaluate the precision of the damage quantification.

6.3. Identification of single damage with different types of response data

Element 7 is assumed to be the only damaged element with a damage extent of 30%. The FE model of the bridge in the undamaged state is known and used as the reference model. As shown in Fig. 6, three measurement points are considered, whose distances from the left support of the bridge are10, 37.5 and 65 m, respectively. The displacement, velocity and acceleration responses at these points are observed and used as the input data for damage identification. The grade-4, grade-5 or grade-6 track irregularity spectra are considered in the train–bridge dynamic interaction analysis. 5% and 10% noises are, respectively, added to the measured train-induced responses. A typical acceleration response of point 2 is shown in Fig. 7. The sampling frequency is 200 Hz, and 1500 forced-vibration response data (NM=1500, from 0.5 to 8 s) are used in the identification.

Listed in Table 2 are the identification results using displacement responses, velocity responses and acceleration responses under the grade-4 track irregularity spectrum. Shown in Fig. 8 are the identified damage indices for different

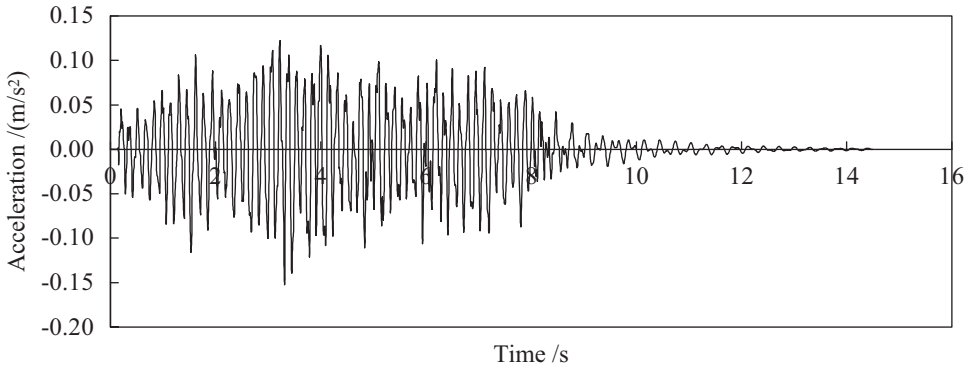

Fig. 7. Acceleration response of the bridge midpoint.

Table 2
Identification results using different types of response.

Point no.	Noise level (%)	Displacement			Velocity			Acceleration		
		RE (%)	α^7 (%)	N_t	RE (%)	α^7	N_t	RE (%)	α^7 (%)	N_t
1	0	0.46	29.86	175	0.76	29.77	66	1.75	29.48	35
	5	2.64	29.20	239	4.9	28.51	69	2.24	29.32	53
	10	3.27	29.01	274	6.6	28.00	216	2.34	29.29	219
2	0	0.89	29.73	232	1.06	29.68	216	1.72	29.48	139
	5	2.11	29.34	275	2.57	29.22	252	4.16	28.74	199
	10	3.47	28.95	325	3.99	28.79	276	4.72	28.57	246
3	0	1.82	29.45	176	1.62	29.51	143	1.49	29.95	129
	5	2.61	29.21	223	2.11	29.36	193	1.98	29.40	156
	10	3.53	28.93	285	3.23	29.02	196	2.87	29.13	229

N_t is the iteration step number of damage index vector.

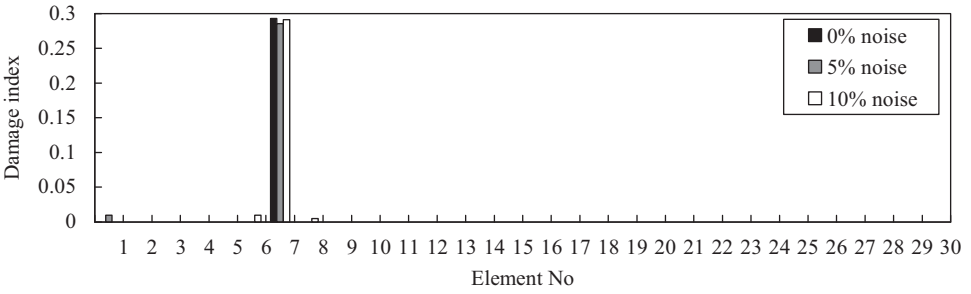

Fig. 8. Damage identification using acceleration responses of point 3 at different noise levels.

noise levels using the acceleration response of point 3. The identified results using the acceleration responses (10% noise) of different measurement points are shown in Fig. 9.

From Table 2, Figs. 8 and 9, it can be concluded that:

(1) The absolute damage of element 7 is well identified either using the polluted displacement responses, velocity responses or acceleration responses.
(2) The identified results using the responses at different noise levels correspond to each other, but the needed number of iterations and the identification error increase slightly with the noise level.
(3) The identified damage using the responses from either of the three points is close to the true value, indicating that the location of the measurement point does not considerably influence the identification result.

Fig. 10 shows the damage indices at different iteration steps using the acceleration response measured at point 3 under the grade-6 track spectrum. It can be seen that the damage indices rapidly converge to their true values. If the purpose is to simply locate the damage, only a few iteration steps are needed.

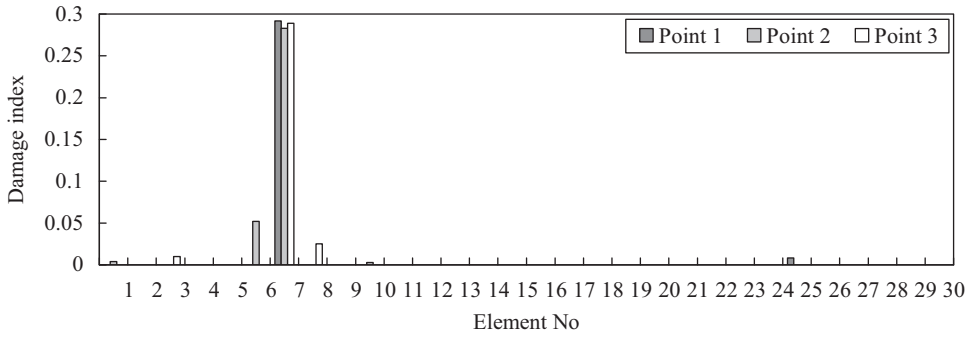

Fig. 9. Damage identification using acceleration responses of different points (10% noise).

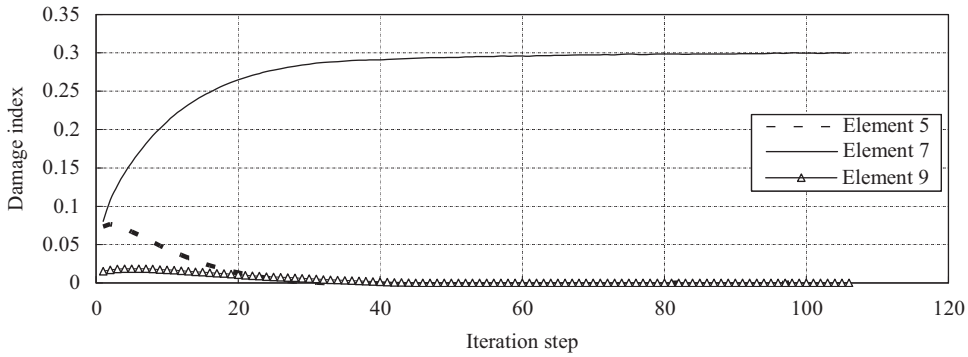

Fig. 10. Damage indices versus iteration step (10% noise).

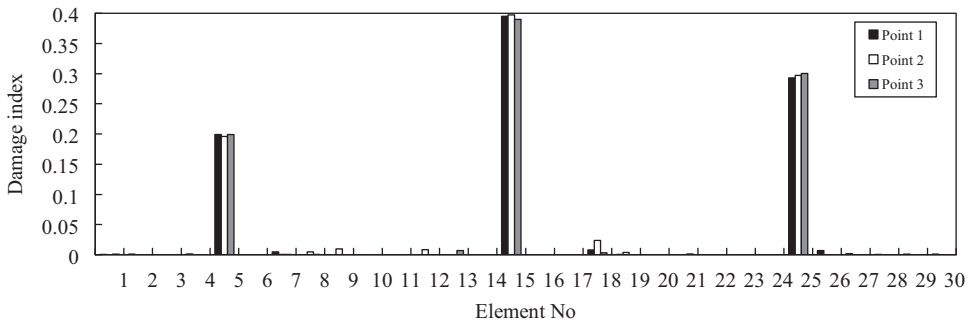

Fig. 11. Identified damage indices using different measurement points (10% noise).

6.4. Identification of multiple damage

In the analysis, the initial FE model of the bridge is known and elements 5, 15 and 25 are assumed to simultaneously suffer damage with extents of 20%, 40% and 30%, respectively. The grade-6 track irregularity is used, and 1%, 5%, and 10% noises are, respectively, added to the measurement responses. The train and the measurement points are the same as in Section 6.3. The acceleration response measured at point 1 with a sampling frequency of 200 Hz is used for damage identification. For signals with noise, 300 response data are used, while 1000 for signals with noise. The identification results using different measurement points are shown in Fig. 11. The identified damage indices using the responses at different noise levels are presented in Fig. 12. The errors between the identified damage indices and the assumed ones are listed in Table 3. Fig. 13 shows the convergence curves of the damage indices.

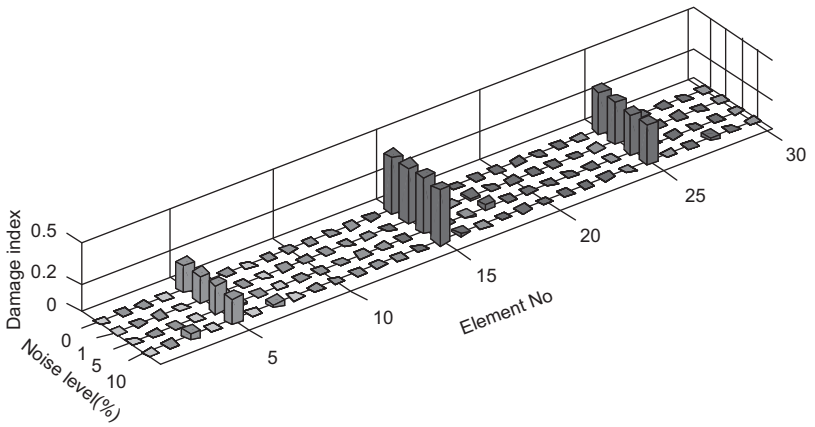

Fig. 12. Identified damage indices using the responses at different noise levels.

Table 3
Identification errors using different measurement points.

Measurement												
Point	1				2				3			
Noise level (%)	0	1	5	10	0	1	5	10	0	1	5	10
RE (%)	1.3	1.4	4.6	6.6	1.9	2.4	4.7	5.4	0.8	2.3	4.8	7.0

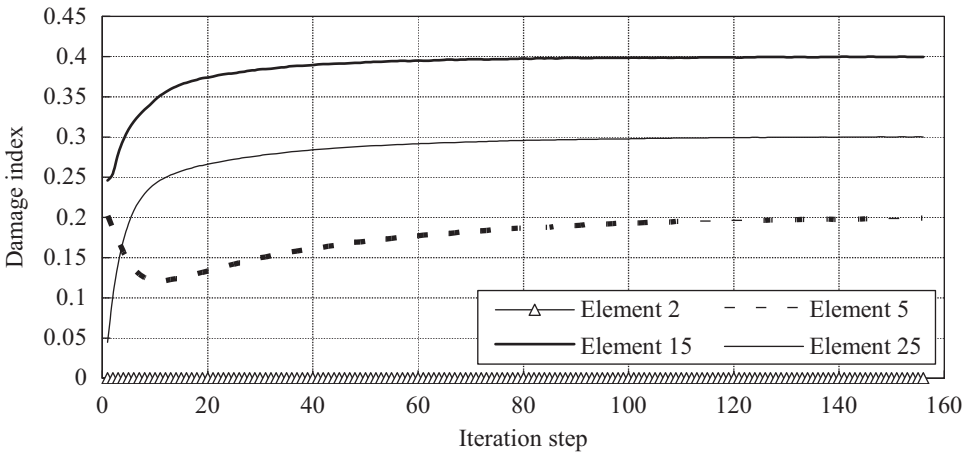

Fig. 13. Damage indices versus iteration step (10% noise).

In order to study the influence of track irregularities on the damage identification results, another damage case is considered, where 30%, 20% and 40% reductions in stiffness are assumed in elements 3, 12 and 28, respectively. Track irregularity spectra with grades from 4 to 6 are used, and 10% noise is added to the calculated responses. Fig. 14 shows the identified results when the track exhibits different grades of irregularity. The errors between the identified damage indices and the assumed ones are listed in Table 4.

From the above results, the following conclusions can be drawn:

(1) The identified absolute damage indices using the responses of different measurement points correspond with each other (see Fig. 11), showing that the location of measurement point does not influence the identification results very much.
(2) The identified results are acceptable when the noise level is up to 10%, which shows that the proposed damage identification method has a good ability of resisting noise (see Fig. 12). However, with the increase of noise levels, the identification errors become somewhat larger.
(3) The damage indices converge quickly at the initial stage, and then change slowly towards the true values (see Fig. 13). If the purpose is to simply locate the damage, only a few iteration steps are needed, saving a lot of computation time.
(4) Although the identification errors increase slightly when the track irregularities become larger, the detected damage is still close to the true value (see Fig. 14), showing that the proposed method is not sensitive to track irregularities.

6.5. Damage identification without tuned FE reference model

If the initial FE model of the bridge in the undamaged state is obtained by the FE model updating technique using test data [34], the identified damage by the proposed method is the absolute one. However, when only the FE model in an already damaged state or in a state with some uncertainties regarding the FE model at time t_1 is identified and taken as the reference model, the identified damage at time t_2 is the damage increment between the two states.

In the analysis, only the damaged state of the bridge at time t_1 is known, in which elements 2, 6, 13 and 23 suffer damage with extents of 0%, 10%, 15% and 10%, respectively. The absolute damage for elements 2, 6, 13 and 23 at time t_2 is assumed to be 10%, 15%, 30% and 20%, respectively.

The train and the measurement points are the same as in Section 6.3. The grade-6 track irregularity spectrum is used and 10% noise is added to the measurement response. The sampling frequency is 200 Hz and 1000 forced-vibration acceleration response data (NM=1000, from 1 to 6 s) of point 1 are used for damage identification. The identified damage increment between time t_1 and t_2 is shown in Fig. 15.

It can be observed from Fig. 15 that:

(1) The sum of the damage in the reference state at time t_1 and the identified damage increase is very close to the true damage at time t_2, showing that the proposed method is also effective for the identification of the damage increase between two different states without prior knowledge of the damage at the first state.

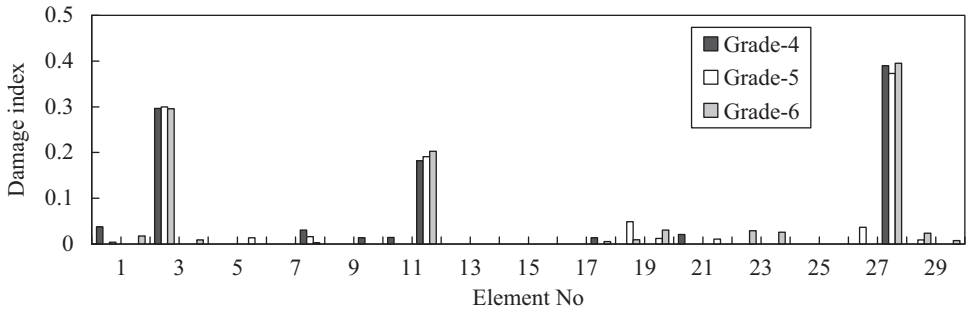

Fig. 14. Identified damage indices under different track irregularity grades (10% noise).

Table 4
Identification errors for different irregularity grades.

Irregularity grade	6		5		4	
Noise level (%)	0	10	0	10	0	10
RE (%)	0.8	6.8	1.3	7.3	2.1	7.8

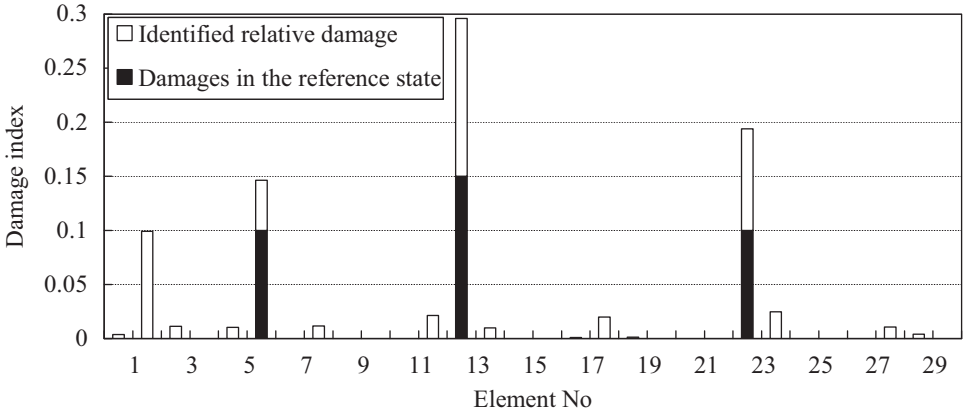

Fig. 15. Relative damage identification (10% noise).

(2) Although the measurement noise level is up to 10%, the assumed 5% and 10% increases of damage at element 6 and element 2 are still well identified, which proves the robustness of the proposed damage identification method.

7. Conclusions and discussions

The following conclusions can be extracted from this paper:

(1) The dynamic responses of the train–bridge system and the sensitivity matrices of the dynamic responses with respect to the damage indices can be calculated by the train–bridge dynamic interaction model. An iterative updating procedure using the train-induced responses and the response sensitivity matrices is proposed to locate and quantify the damages of railway bridges.
(2) Only one measurement point is needed to detect the relative or absolute damage of the bridge. The location of the measurement point does not influence the identified results much.
(3) The proposed damage identification method has a rather good stability against measurement noise. The identified results are acceptable even for a noise level up to 10%.
(4) The proposed damage identification method is insensitive to the track irregularity.

Although the efficacy of the proposed damage identification method is good in theory, when it is used in practice, the following aspects should be considered:

(1) The considered train should be the same and run at the same speed before and after the bridge is damaged to ensure that the loads acting on the bridge are the same.
(2) Disturbing environmental influences, such as wind and temperature, must be minimized. For example, the experiment should be conducted under similar wind speed and temperature conditions before and after the bridge is damaged.

Acknowledgements

The research of this project was partly supported by the Natural Science Foundation of China (Grant no. 51078029), the Fundamental Research Funds for the Central Universities (Grant no. 2009JBM061) and the Flanders-China Bilateral Project (BIL 07/07).

References

[1] P. Cawley, R.D. Adams, The location of defects in structures from measurements of natural frequencies, *Journal of Strain Analysis* 14 (2) (1979) 49–57.
[2] O.S. Salawu, Detection of structural damage through changes in frequency: a review, *Engineering Structures* 19 (9) (1997) 718–723.
[3] J.M. Ndambi, J. Vantomme, K. Harri, Damage assessment in reinforced concrete beams using eigenfrequencies and mode shape derivatives, *Engineering Structures* 24 (2002) 501–515.
[4] Z. Ismail, H. Abdul Razak, A.G. Abdul Rahman, Determination of damage location in RC beams using mode shape derivatives, *Engineering Structures* 28 (2006) 1566–1573.
[5] A.K. Pandey, M. Biswas, M.M. Samman, Damage detection from change s in curvature mode shape, *Journal of Sound and Vibration* 145 (2) (1991) 321–332.
[6] R.O. Curadelli, J.D. Riera, D. Ambrosini, M.G. Amani, Damage detection by means of structural damping identification, *Engineering Structures* 30 (2008) 3497–3504.
[7] Z.Y. Shi, S.S. Law, Structural damage localization from modal strain energy change, *Journal of Sound and Vibration* 218 (5) (1998) 825–844.

[8] X. Liu, N.A.J. Lieven, P.J. Escamilla-Ambrosio, Frequency response function shape-based methods for structural damage localization, *Mechanical Systems and Signal Processing* 23 (2009) 1243–1259.
[9] C. Farhat, F.M. Hemez, Updating finite element dynamic models using an element-by-element sensitivity methodology, *AIAA Journal* 31 (1993) 1702–1711.
[10] D. Wu, S.S. Law, Model error correction from truncated modal flexibility sensitivity and generic parameters. I: simulation, *Mechanical Systems and Signal Processing* 18 (6) (2004) 1381–1399.
[11] S.W. Doebling, C.R. Farrar, M.B. Prime, D.W. Shevitz, A review of damage identification methods that examine changes in dynamic properties, *Shock and Vibration Digest* 30 (2) (1998) 91–105.
[12] T. Zou, L. Tong, G.P. Steve, Vibration based model-dependent damage (delamination) identification and health monitoring for composite structures: a review, *Journal of Sound and Vibration* 230 (2) (2000) 357–378.
[13] G.W. Housner, L.A. Bergman, T.K. Caughey, Structural control: past, present, and future, *Journal of Engineering Mechanics—ASCE* 123 (9) (1997) 897–971.
[14] M.I. Friswell, J.E. Mottershead, *Finite Element Model Updating in Structural Dynamics*, Kluwer Academic Publishers, Dordrecht, 1996.
[15] M.M. Abdel Wahab, G. De Roeck, B. Peeters, Parameterization of reinforced concrete structures using model updating, *Journal of Sound and Vibration* 228 (4) (1999) 717–730.
[16] G.R. Liu, S.C. Chen, A novel technique for inverse identification of distributed stiffness factor in structures, *Journal of Sound and Vibration* 254 (5) (2002) 823–835.
[17] J. Cattarius, D.J. Inman, Time domain analysis for damage detection in smart structures, *Mechanical Systems and Signal Processing* 11 (3) (1997) 409–423.
[18] J. Chen, J. Li, Simultaneous identification of structural parameters and input time history from output-only measurements, *Computational Mechanics* 33 (5) (2004) 365–374.
[19] T. Shi, N.P. Jones, J. Hugh Ellis, Simultaneous estimation of system and input parameters from output measurements, *Journal of Engineering Mechanics—ASCE* 126 (7) (2000) 746–753.
[20] X.L. Ling, P.E. Achintya Haldar, Element level system identification with unknown input with Rayleigh damping, *Journal of Engineering Mechanics—ASCE* 130 (8) (2004) 877–885.
[21] Z.R. Lu, S.S. Law, Features of dynamic response sensitivity and its application in damage detection, *Journal of Sound and Vibration* 303 (2007) 305–329.
[22] Z.R. Lu, J.K. Liu, M. Huang, W.H. Xu, Identification of local damages in coupled beam systems from measured dynamic responses, *Journal of Sound and Vibration* 326 (2009) 177–189.
[23] L. Majumder, C.S. Manohar, A time domain approach for damage detection in beam structures using vibration data with a moving oscillator as an excitation source, *Journal of Sound and Vibration* 268 (2003) 699–716.
[24] X.Q. Zhu, S.S. Law, Damage detection in simply supported concrete bridge structures under moving vehicular loads, *Journal of Vibration and Acoustics—Transactions of the ASME* 129 (1) (2007) 58–65.
[25] R.W. Clough, J. Penzien, *Dynamics of Structures*, third ed., Computers & Structures, Inc., Berkeley, USA, 2003.
[26] H. Xia, N. Zhang, *Dynamic Interaction of Vehicles and Structures*, Science Press, Beijing, 2005 (in Chinese).
[27] N. Zhang, H. Xia, W.W. Guo, Vehicle–bridge interaction analysis under high-speed trains, *Journal of Sound and Vibration* 309 (2008) 407–425.
[28] R.D. Cook, D.S. Malkus, M.E. Plesha, *Concepts and Applications of Finite Element Analysis*, fourth ed., Wiley, New York, 2001.
[29] M.I. Friswell, J.E. Mottershead, *Finite Element Model Updating in Structural Dynamics*, Kluwer Academic Publishers, Dordrecht, Netherlands, 1995.
[30] A.M. Tikhonov, On the solution of ill-posed problems and the method of regularization, *Soviet Mathematics* 4 (1963) 1035–1038.
[31] P.C. Hansen, Regularization tools—a Matlab package for analysis and solution of discrete ill-posed problem, version 4.1, 2008.
[32] K. Liu, G. De Roeck, G. Lomabaert, The effect of dynamic train–bridge interaction on the bridge response during a train passage, *Journal of Sound and Vibration* 325 (2009) 240–251.
[33] Z. Anis, J.K. Hedrick, Characterization of rail track irregularities, US Department of Transportation, Report No. 1206, 1977.
[34] A. Teughels, J. Maeck, G. De Roeck, Damage assessment by FE model updating using damage functions, *Computers and Structures* 80 (25) (2002) 1869–1879.